# Toothbrushing Region Detection Using Three-Axis Accelerometer and Magnetic Sensor

Young-Jae Lee, *Student Member, IEEE*, Pil-Jae Lee, Kyeong-Seop Kim, Wonse Park, Kee-Deog Kim, Dosik Hwang, and Jeong-Whan Lee*, *Member, IEEE*

***Abstract*—Due to the possible occurrence of periodontal disease at an early age, it is important to have proper toothbrushing habits as early as possible. With this aim, the feasibility and concept of a smart toothbrush (ST) capable of tracing toothbrushing motion and orientation information was suggested. In this study, we proposed the advanced ST system and brushing region classification algorithm. In order to trace the brushing region and the orientation of a toothbrush in the mouth, we required the absolute coordinate information of ST. By using tilt-compensated azimuth (heading) algorithm, we found the inclination and orientation information of the toothbrush, and the orientation information while brushing inner tooth surfaces showed specific heading features that could be reliably discriminated from other brushing patterns. In order to evaluate the feasibility of clinical usage of the proposed ST, 16 brushing regions were investigated by 15 individual healthy subjects. The proposed ST system demonstrated 97.1%($\pm$0.91) of the region detection accuracy and 15 brushing regions could be classified. This study also showed that the proposed ST system may be helpful for dental care personnel in patient education and instruction for oral hygiene regarding brushing habits.**

***Index Terms*—Accelerometer, magnetic sensor, oral hygiene, pattern classification, toothbrush, toothbrushing patterns, toothbrushing regions.**

## I. Introduction

RECENTLY, ubiquitous or pervasive healthcare [1] has emerged as a solution to handle the crisis in the healthcare industry, including skyrocketing costs, a growing incident of medical errors, and the lack of insurance coverage in rural and underserved urban areas. Now, those within the healthcare industry are under increasing pressure to provide better service to more people using limited financial and human resources. Based on these trends, healthcare technologies are now evolving to reduce long-term healthcare costs and improve quality of life [2].

Among various diseases depending on lifestyle, gingivitis and tooth decay are diseases, which require preventive measures and techniques. Nevertheless, even in the adult, inadequate toothbrushing styles can cause dental problems such as chronic gingivitis, gum disease, and so forth. There have been many convenient and automatic electronic toothbrushes available in the market; however, there are some skeptical points regarding efficacy and safety of electronic toothbrushes [3]. Recent studies showed that toothbrushing forces [4]–[9] did not provide effective and qualitative ways of evaluating brushing styles such as motions of the brush head and the minimal duration of brushing, where it should be done, and so on. Therefore, it would be beneficial to the community in terms of both healthcare and economics if we could prevent dental health from deteriorating into worse conditions in the early stages. Improvement in educating society about dental health would reduce healthcare costs and improve quality of life.

The concept of a smart toothbrush (ST) system capable of tracing brushing motion with respect to the dental arches was first proposed and described [10], [11]. From these preliminary studies, we found that the orientation of toothbrush provides distinguishable information such as the roll and heading angles of the toothbrush. The most important problem was the absolute heading information of the toothbrush with respect to a bust mirror in front of the examinee [11]. Even though we might restrict a rotational movement of the head, the location and the orientation of the human body while brushing one's teeth are unpredictable. Thus, we need to estimate the absolute heading information of toothbrush. This kind of problem was well defined and explored in navigational devices in the telematics.

The heading (azimuth) angle is defined as the angle between the North Pole and the direction of movement. Estimation of heading angle could be found in gyrocompassing [12], [13], GPS application [14], and magnetometry using a magnetic compass [15], [16]. Also, if we used gyro sensor for calculating the azimuth angle, the initial azimuth value and the gyro bias problem would impose another complexity in our application. Therefore, if a two-axis magnetic sensor is placed on the horizontal plane, which is parallel with the Earth's surface, the heading angle of the ST could be calculated accurately. Otherwise, a tilt error in the heading angle would be introduced.

Manuscript received June 5, 2011; revised September 5, 2011, and October 26, 2011; accepted November 27, 2011. Date of publication December 22, 2011; date of current version February 17, 2012. This work was supported by the National Research Foundation of Korea funded by the Korea government (MEST) under Grant 2010-0027674. *Asterisk indicates corresponding author.*

Y. J. Lee, P. J. Lee, and K. S. Kim are with the School of Biomedical Engineering, College of Biomedical & Health Science, Konkuk University, Chung-Ju 143-701, Korea (e-mail: zetzlyj@gmail.com; 4265623@naver.com; kyeong@kku.ac.kr).

W. Park and K. D. Kim are with the Department of Advanced General Dentistry, College of Dentistry, Yonsei University, Seoul 120-752, Korea (e-mail: wonse@yuhs.ac; kdkim@yuhs.ac).

D. Hwang is with the School of Electrical and Electronic Engineering, Yonsei University, Seoul 120-749, Korea (e-mail: dosik.hwang@yonsei.ac.kr).

*J. W. Lee is with the School of Biomedical Engineering, College of Biomedical & Health Science, Research Institute of Biomedical Engineering, Konkuk University, Chung-Ju 143-701, Korea (e-mail: jwlee95@kku.ac.kr).

Color versions of one or more of the figures in this paper are available online at http://ieeexplore.ieee.org.

Digital Object Identifier 10.1109/TBME.2011.2181369

Recently, a heading angle estimation technique using magnetic compass was investigated [17], [18]. In this technique, they considered the Earth's dip angle, a slant angle of a compass needle, to compensate the tilt error. This means that the magnetic field is parallel to the Earth's magnetic field around the equator, but begins to slant to the Earth core as the latitude is increased. This phenomenon would be a major problem in global navigation systems, but as to the ST system, the local activity area of ST is so small that this phenomenon is negligible. Nonetheless, we need to consider the latitude information, where the toothbrush is used in order to reduce the heading angle error. In the ST coordinate system, the heading is considered as the direction of the radial axis of ST with respect to the $x$-axis of the world frame coordinate.

Another problem, not as critical as the absolute heading information, is the ambiguity of ST heading angles while brushing at inner tooth surfaces. For example, when brushing at the maxillary left molar buccal side and maxillary right molar lingual side, the heading information of each ST seems to be difficult to discriminate from one another in a real-time mode. The same situation occurs while brushing at maxillary right molar buccal side and maxillary left molar lingual side. While brushing these ambiguous regions, we found that the heading angle of ST is slightly different from one other because of a space where the head of toothbrush is supposed to be placed in lingual side. This small change of the heading angle enables us to recognize brushing regions using a pattern classification method effectively. Also, as to the problem of body movement during toothbrushing, we only considered the scenario in which the body of examinees was static, i.e., maintaining the initial posture toward wall mirror. If the factor of body movement is included, other classification criteria such as vision features would be necessary to include.

In this paper, we will briefly describe an implementation of the ST. We will describe how toothbrush posture is recognized in real time, and how toothbrushing regions are classified using a pattern classification algorithm. In order to assess the feasibility for clinical application of the proposed ST, 16 possible toothbrushing, as illustrated in Fig. 1, were investigated. As to toothbrushing regions, it is somewhat difficult to locate the toothbrushing regions, which are certified or confirmed by the dentist and dental hygienist. Although in the American Dental Association and American Dental Hygienists' Association, four or six brushing regions known as quadrant and sextant as follows:

1) Inner and outer tooth surfaces of molar (no indication of left or right and maxilla or mandible).
2) Anterior buccal (AB) and lingual sides of the front teeth (no indication of maxilla or mandible).
3) Chewing surfaces of the teeth (molar occlusal—no indication of left or right and maxillary or mandible).
4) Tongue (not considered in our study).

These regions are generally accepted in the dental community. But it is difficult to find any quantitative index in order to assess the quality of toothbrushing. Therefore, we discussed and extended brushing regions to 16 regions considering functions of the proposed ST system and the symmetry of the dental arc.

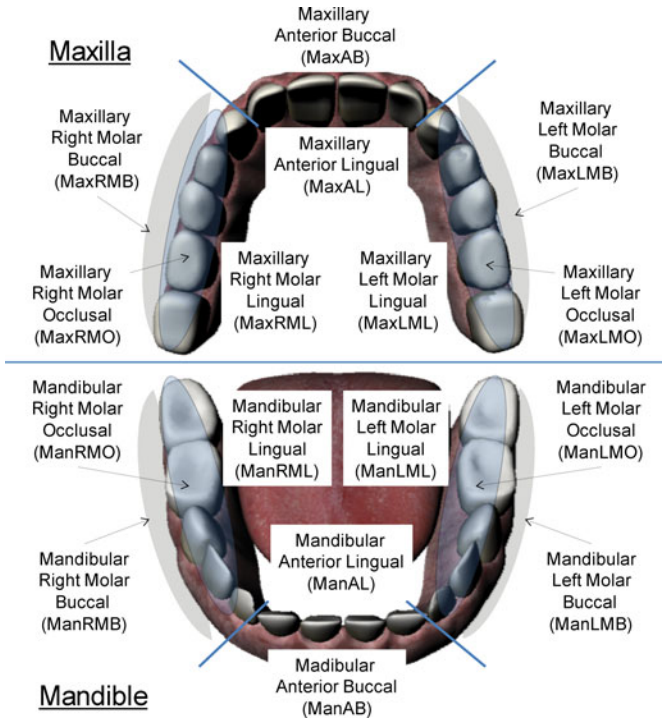


Fig. 1. Possible toothbrushing regions in an oral cavity.

## II. Methods

### A. Implementation of ST

The heading information of ST was measured using magnetic field sensors. There are several types of magnetic sensors such as fluxgate, magnetoresistive, and magnetoinductive. A common type of magnetic sensor for navigation systems is the fluxgate sensor. But, it tends to be bulky, somewhat fragile, and has a slow response time, 2–3 s. A magnetic sensor based on magnetoinductive technique has better characteristics in terms of power consumption and stability over temperature than fluxgate and magnetoresistive sensors. However, because of its inherent solenoid coil mechanical structure, a magnetoinductive sensor tends to be bulky and fragile. In contrast, anisotropic magnetoresistive (AMR)-based magnetic sensor has well-defined axis of sensitivity and can be mass produced in a small solid-state package, along with a fast response time of less than 1 $\mu$s. Fig. 2 shows the implemented ST, and Fig. 3 shows the related coordinate of ST and the reference coordinate of the dental arc. Fig. 4 illustrates the definition of ST posture, UP, DOWN, LEFT, and RIGHT. The electrical and mechanical specifications of the proposed ST system are summarized in Table I.

### B. Toothbrush Posture Angles; Tilt Compensation

Backward and forward movements of ST were measured by the three-axis accelerometers (MMA7260QT, Freescale, TX). The sensitivity of the accelerometer was set to 800 mV/g. The dc and ac components of the accelerometer were used to measure the inclination information and activity level of the toothbrush using IIR filters. A low-pass filter (LPF, sixth order, Butterworth, cascade transposed IIR) was designed and implemented

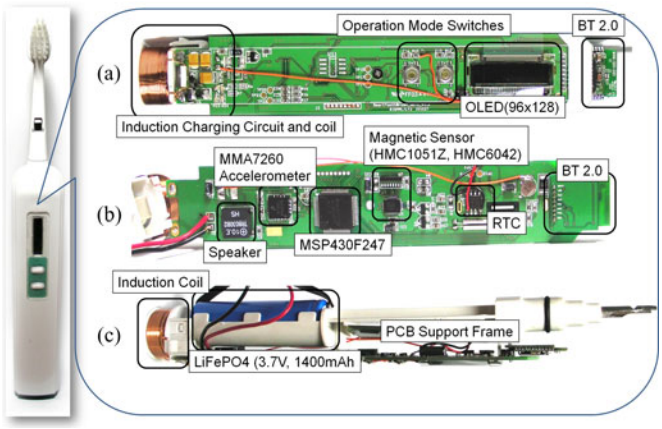


Fig. 2. System configuration of our proposed smart toothbrushing. (a) Top side. (b) Bottom side of ST system PCB. (c) Lateral view of PCB support frame.

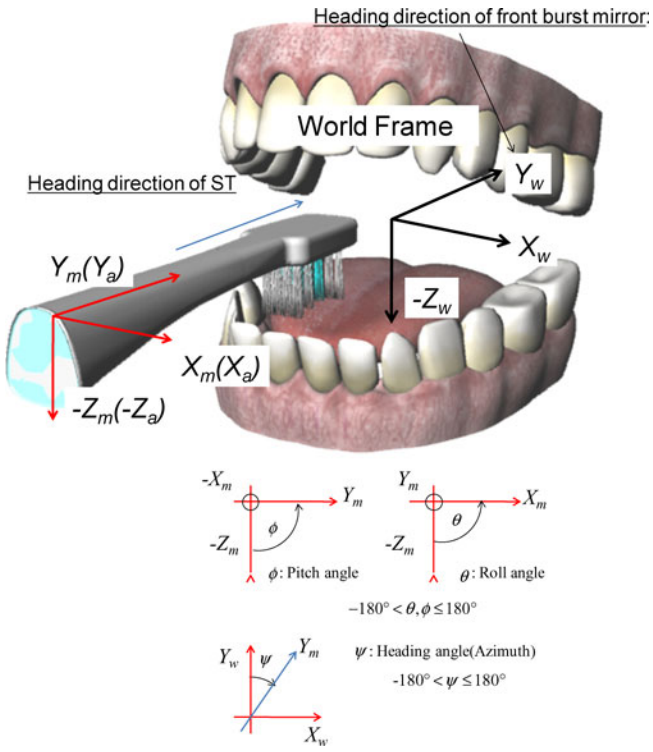


Fig. 3. Relationship between the smart toothbrush coordinate and the world coordinate.

in MSP430 MCU in order to pass the slow dc components, which are related to the gravitational force. A high-pass filter (HPF, sixth order, Butterworth, cascade transposed IIR) was to pass the ac component, which is related with brushing activities. DC components of the acceleration signals are related to the gravitational force exerted on the toothbrush and ac components are related with the brushing motions.

During our experiments, we observed that a dc component does not exceed 2 Hz, and ac frequency components are higher than 3 Hz. Thus, we set the cutoff frequency of LPF to 2 Hz and that of HPF to 3 Hz, considering the phase response and roll-off characteristics of IIR filters. The coefficients of IIR filters were

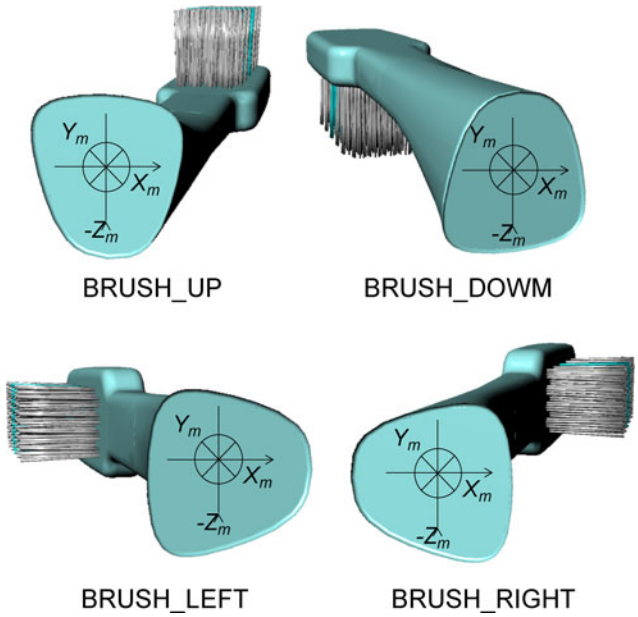


Fig. 4. Definition of toothbrush postures, UP, DOWN, LEFT, and RIGHT.

TABLE I
ELECTRICAL AND MECHANICAL SPECIFICATION OF THE PROPOSED SMART TOOTHBRUSH SYSTEM

| | | Specification |
|---|---|---|
| Degree of Freedom (DOF) | | 6 |
| Accelerometer (MMA7260) | | 3-axis(800 mV/g) |
| Magnetic Sensor (HMC6042) | | 2-axis(1.0 mV/V/gauss) |
| Magnetic Sensor (HMC1051Z) | | 1-axis (1.0 mV/V/gauss) |
| A/D converter (embedded in MSP430F247) | Resolution | 12 bits |
| | Sampling rate | 60-Hz |
| Wireless Communication | Bluetooth V2.0 + EDR Class II ( 20mA @ standby/ 37mA @ Tx/Rx) Serial Port Profile (SPP) | |
| Battery | $LiFePO_4$ (3.7V) | 1400 mAh |
| Physical Characteristics | Size (W x H x D) | 170x23x20 mm |
| | Weight | 46 g |
| Current consumption | | Approx. 45 mA @ 3.3V |

implemented in double-precision floating-point format coded in C-language, Code Composer Studio v4 (CCS V4.3, Texas Instruments, Dallas, TX). After LPF and HPF filtering, the roll ($\theta$) and pitch ($\varphi$) angles of ST were calculated as follows:

$$\theta = \arcsin\left(\frac{\bar{X}_a}{g}\right) \tag{1}$$

$$\phi = \arcsin\left(\frac{-\bar{Y}_a}{g\cos\theta}\right) \tag{2}$$

where $\bar{X}_a$ and $\bar{Y}_a$ indicate the low-pass filtered and normalized output of the $x$- and $y$-axis of accelerometer, respectively, and $g$ is the gravity acceleration (9.8 ms/s$^2$).

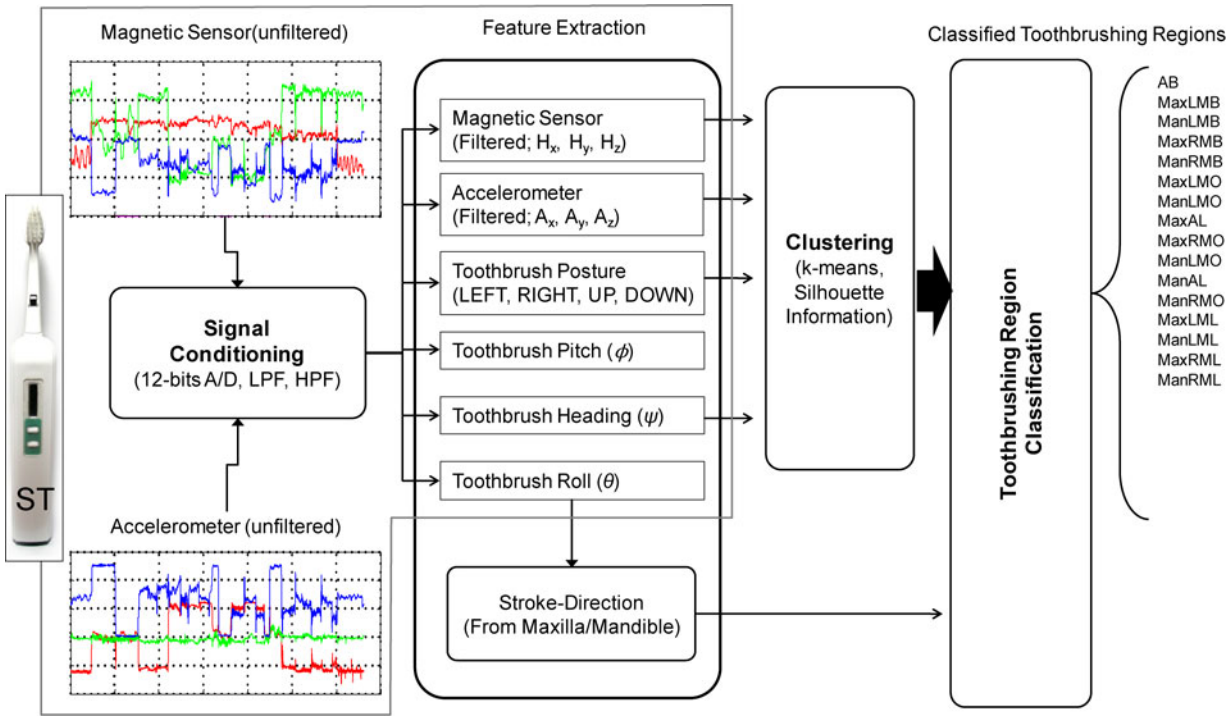


Fig. 5. Block diagram of classification processes for toothbrushing regions.

### C. Heading (Azimuth) Angle Estimation

As for the orientation information of ST, we used AMR-based magnetic sensors (HMC6042, HMC1051Z, Honeywell, Minneapolis, MN) because of its fast response time. At first, the magnetic sensor signals were filtered by the same LPF, which was used for acceleration signals. Then, filtered magnetic signals were normalized as follows:

$$\bar{X}_m = (X_m - \mathrm{Bias}_x)\,\mathrm{SF}_x \tag{3}$$

$$\mathrm{Bias}_x = \frac{(X_{m\_\max} + X_{m\_\min})}{2} \tag{4}$$

$$\mathrm{SF}_x = \frac{2\cos\lambda}{(X_{m\_\max} - X_{m\_\min})} \tag{5}$$

where $X_m$ is the filtered output of the magnetic sensor, $\bar{X}_m$ is the normalized $x$-axis magnetic sensor, and $X_{m\_\max}$, $X_{m\_\min}$ are the maximum and minimum values of the filtered output of the magnetic sensors on a horizontal plane, respectively. Here, $\mathrm{Bias}_x$ denotes the bias of the $x$-axis magnetic sensor and $\mathrm{SF}_x$ is the scale factor of $x$-axis of magnetic sensor [18]. $\lambda$ is a dip angle, which varies with the latitude. The latitude of our campus is approximately 56.9° and calculated with latitude information by

$$\lambda = \tan^{-1}(2\tan L) \tag{6}$$

where $L$ denotes the latitude. The normalization of the $y$- and $z$-axis of the magnetic sensor was performed by the same process.

The heading (azimuth) angle was estimated as follows [18]:

$$\psi = \tan^{-1}\left(\frac{-\bar{Y}_m\cos\phi + \bar{Z}_m\sin\phi}{\bar{X}_m\cos\theta + \bar{Y}_m\sin\theta\sin\phi + \bar{Z}_m\sin\theta\cos\phi}\right) \tag{7}$$

where $\theta$, $\phi$, and $\psi$ indicate roll, pitch, and heading (azimuth) angle, respectively.

In addition to the heading angle of ST with respect to the North Pole, the heading direction of the wall mirror is measured using the ST since toothbrushing regions are classified with respect to the front wall mirror. The initial heading direction of the front wall mirror was used as an offset angle to calculate the heading angle of ST with respect to the front wall mirror.

### D. Toothbrushing Region Classification

Fig. 5 shows a block diagram of the proposed toothbrushing region algorithm. Toothbrush motions were considered as having two categories, posture and orientation. The posture information included the roll and pitch angles of ST with respect to the horizontal plane. The orientation information of ST included the heading angle with respect to the direction of bust mirror in front of the examinee. The posture of ST is classified into four positions, BRUSH_RIGHT, BRUSH_LEFT, BRUSH_DOWN, and BRUSH_UP defined by

$$\text{Posture} = \begin{cases} -45 \le \theta < 45\,\&\,\text{Activity} > \text{Th} \Rightarrow \text{BRUSH\_LEFT} \\ 45 \le \theta < 135\,\&\,\text{Activity} > \text{Th} \Rightarrow \text{BRUSH\_UP} \\ 135 \le \theta < -135\,\&\,\text{Activity} > \text{Th} \Rightarrow \text{BRUSH\_RIGHT} \\ -135 \le \theta < -45\,\&\,\text{Activity} > \text{Th} \Rightarrow \text{BRUSH\_DOWN} \end{cases} \tag{8}$$

where

$$\text{Activity} = \left(|dAX\text{var}|^2 + |dAY\text{var}|^2 + |dAZ\text{var}|^2\right)^{1/2}$$

Here $\theta$ is the roll angle of ST, and $dAX\text{var}$, $dAY\text{var}$, and $dAZ\text{var}$ are the variance of each accelerometer axis. Posture classification is done seamlessly while the activity of ST is above the threshold (Th = 130 mg/LSBs).

The orientation of ST, heading information, also could be estimated in real-time using (7). But this absolute heading information is quite vulnerable to the head movement while toothbrushing even though the motion of subject's head is restricted. Also, another factor, which could affect the heading angle of ST, is the geographical location, where toothbrushing is done since in real life the experiment location is quite variable. Thus, we have to not only use the absolute heading information of ST as a seed of brushing pattern classification, but also the relative heading information of ST. As a relative criterion for classification, we used the filtered raw magnetic sensor signals, accelerometer signals, and the heading information combined. Then, we formed a feature vector $\mathbf{A}$ ($n \times 7$) as follows:

$$\mathbf{A} = [\mathbf{a}_1, \mathbf{a}_2, \ldots, \mathbf{a}_N]^T = [\mathbf{X}_m, \mathbf{Y}_m, \mathbf{Z}_m, \mathbf{X}_a, \mathbf{Y}_a, \mathbf{Z}_a, \mathbf{H}]$$

where

$$\begin{aligned}
\mathbf{X}_m &= [\bar{X}_m(1), \bar{X}_m(2), \ldots, \bar{X}_m(N)]^T, \\
\mathbf{X}_a &= [\bar{X}_a(1), \bar{X}_a(2), \ldots, \bar{X}_a(N)]^T \\
\mathbf{Y}_m &= [\bar{Y}_m(1), \bar{Y}_m(2), \ldots, \bar{Y}_m(N)]^T, \\
\mathbf{Y}_a &= [\bar{Y}_a(1), \bar{Y}_a(2), \ldots, \bar{Y}_a(N)]^T, \\
\mathbf{Z}_m &= [\bar{X}_m(1), \bar{X}_m(2), \ldots, \bar{X}_m(N)]^T, \\
\mathbf{Z}_a &= [\bar{Z}_a(1), \bar{Z}_a(2), \ldots, \bar{Z}_a(N)]^T \\
\mathbf{H} &= [\text{Heading}(1), \text{Heading}(2), \ldots, \text{Heading}(N)]^T. \qquad (9)
\end{aligned}$$

The number of row $N$ depends on the number of samples in the segment classified by posture classification (8).

Each segment represents the posture of ST, and contains magnetic and accelerometer sensor signals, which points at different directions. This means that ST is in the BRUSH_LEFT position while brushing at left molar buccal side and right molar lingual side of maxilla and mandible. The same situation occurs while brushing at the right molar buccal side and left molar lingual side of maxilla and mandible. If we looked closer at the magnetic sensor signals, we found a slight difference between magnetic axes. This makes different heading angle of ST. This characteristic seems to be caused by the space, where the head of the toothbrush is placed on the lingual side. When brushing at molar buccal sides, the head of ST would be placed at a cheek as close as possible. But, when brushing at molar palatal sides, the head of ST is placed on the lingual side, and in this position, a room for bristle movement is needed toward the tongue. Also, these differences allow us to estimate the position of ST.

Thus, classified posture segments of ST are fed into further classification process. In order to classify the posture segment in more depth, we used a $k$-means clustering algorithm [19] since it is one of the computationally light and unsupervised learning algorithms.

We let $\mathbf{c}_j$ be the mean of the feature vectors in the brushing region cluster $j$. If the region clusters are well separated, a minimum-distance classifier, such as Euclidean distance $\|\mathbf{a}_i - \mathbf{c}_j\|$would be minimized. The metric function $D$ as a measure of distortion is defined by

$$D = \sum_{j=1}^{k}\sum_{i=1}^{N} \|\mathbf{a}_i - \mathbf{c}_j\| = \sum_{j=1}^{k}\sum_{i=1}^{N} \sqrt{(\mathbf{a}_i - \mathbf{c}_j)^T(\mathbf{a}_i - \mathbf{c}_j)} \qquad (10)$$

where $k$ is the desired number of bushing region clusters and $N$ is number of samples in the selected posture segment. If $k$ is given, iterative procedure of $k$-means algorithm repeat until following condition is met:

$$\Delta D = \frac{D_{\text{previous}} - D_{\text{current}}}{D_{\text{previous}}} < 10^{-4}. \qquad (11)$$

As previously mentioned, each posture segment of ST motion might include different orientations. Therefore, we could not definitively decide the number of subsegment brushing regions. In order to identify the number of brushing region cluster sets in the selected posture segment of ST motion, which are compact and well separated, silhouette validation method [20] was used.

Using this method, each candidate cluster $i$ could be represented by silhouette information value $S^{(i)}(\cdot)$, which is based on the comparison of its tightness and separation for each cluster and a total data set. The average silhouette value was tested for evaluation of clustering validity. If silhouette value is close to 1, it means that the sample is well clustered and it was assigned to a very appropriate cluster. The optimal number of clusters $k$ is decided by the following:

$$\eta = \max_{i=2\ldots5} \sum_{j=1}^{N} \frac{S^{(i)}(j)}{N}$$
$$k = \begin{cases} i, & \text{if } \eta > 0.7 \\ 1, & \text{if } \eta \le 0.7 \end{cases} \qquad (12)$$

where $S^{(i)}(\cdot)$ is the silhouette value when the number of cluster is $i$ and $N$ is number of samples in the selected posture segment. Each subsegment of ST motions clustered by the optimal number of clusters was then assigned to toothbrushing regions based on the heading information, as summarized in Table II.

### *E. Toothbrushing Experiments and Protocol*

In order to collect toothbrushing patterns and evaluate the performance of the proposed toothbrushing region classification algorithm, 15 volunteers (11 males and 4 females, mean age 23 $\pm$ 2 years, 13 right handed and 2 left handed) who had no dental disease and no undergoing orthodontic treatments participated in our experiment. Prior to the toothbrushing, each subject was educated on the brushing sequences, as shown in Fig. 6. All subjects were asked to stay in motion at least 5 s at each brushing region. Brushing motion of ST at outer and inner tooth surfaces was assumed to be rolling stroke method [21]. The ST was placed parallel to the tooth so that the bristles were pointing apically, upward for the maxillary arch and downward for the

TABLE II
DECISION CRITERIA FOR THE CLASSIFICATION OF TOOTHBRUSHING REGIONS

| Posture | Heading angle H (deg) | Rolling –Stroke Direction | Toothbrushing regions | Cluster Name |
|---|---|---|---|---|
| BRUSH LEFT | 170 ≤ H< 190 | X | (Maxillary/Mandibular) Anterior Buccal side [* Initial start location (Left-handed) ] | AB |
| | 80 ≤ H< 110 | From Maxilla | Maxillary Left Molar Buccal side | MaxLMB |
| | | From Mandible | Mandibular Left Molar Buccal side | ManLMB |
| | 60 ≤ H< 80 | From Maxilla | Maxillary Right Molar Palatal side | MaxRMP |
| | | From Mandible | Mandibular Right Molar Palatal side | ManRMP |
| BRUSH RIGHT | 350 ≤ H< 10 | X | (Maxilla/Mandible) Anterior Buccal side [* Initial start location (Right-handed) ] | AB |
| | 80 ≤ H< 110 | From Maxilla | Maxillary Right Molar Buccal side | MaxRMB |
| | | From Mandible | Mandibular Right Molar Buccal side | ManRMB |
| | 120 ≤ H < 110 | From Maxilla | Maxillary Left Molar Palatal side | MaxLMP |
| | | From Mandible | Mandibular Left Molar Palatal side | ManLMP |
| BRUSH DOWN | 80 ≤ H< 110 | X | Mandibular Anterior Lingual side | ManAL |
| | 55 ≤ H < 80 | X | Mandibular Right Molar Occlusal side | ManRMO |
| | 110 ≤ H< 135 | X | Mandibular Left Molar Occlusal side | ManLMO |
| BRUSH UP | 80 ≤ H< 110 | X | Maxillary Anterior Lingual side | MaxAL |
| | 55 ≤ H < 80 | X | Maxillary Right Molar Occlusal side | MaxRMO |
| | 110 ≤ H< 135 | X | Maxillary Left Molar Occlusal side | MaxLMO |

H = the heading angle of ST with respect to the *x*-axis of the world coordinates.
X = Don't care.

mandibular arch. At molar occlusal sides, brushing motion was assumed to be a simple scrubbing method.

The ST was placed at a right angle to the tooth occlusal surface and the brush was moved with back and forth scrubbing strokes. Throughout the toothbrushing period, an inspector at the receiving computer side pressed a keyboard whenever toothbrushing regions had changed. These time-event signals were recorded at the same time with transmitted sensor signals and used as the time-event reference in order to calculate the time period of toothbrushing at each region. All the subjects participated in the experiment provided written informed consent forms prior to beginning experiments.

## III. RESULTS

### A. Accuracy Tolerance of ST

A series of experiments were carried out in order to validate the accuracy tolerance of the estimated roll, pitch, and heading angles by the ST using a specially designed calibration system, as shown in Fig. 7. Roll, pitch, and heading angles of the calibrator frame were controlled with a computer through stepping motor drivers. The calibrator frames repeated predefined angles or positions until interrupted by the user. Then, sensor signals

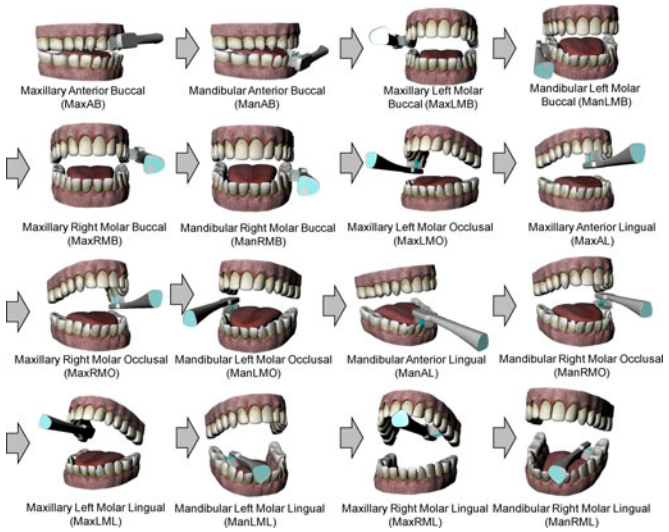


Fig. 6. Toothbrushing sequences. The sequence is determined without any clinical implications, but for the convenience of processing.

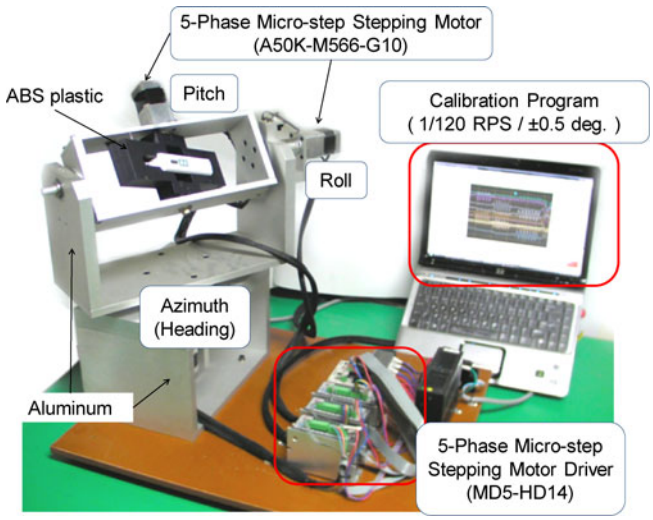


Fig. 7. Calibration system for accelerometer and magnetic sensors. The system was manipulated by a special control program, which repeats the predefined rotation sequences, roll, pitch, and azimuth angles from −180° to 180°. Sensor signals were transmitted to a computer wirelessly and the calibration coefficients for normalization were stored in memory in the ST system PCB.

and estimated angles were transmitted to the computer using a Bluetooth communication module.

The calibrator frames consisted of two materials, aluminum and acrylonitrile butadiene styrene (ABS) plastic. The body, which controls the pitch angle, was made of ABS plastic since this frame is close to the magnetic sensor module. Here, stepping motors do not affect on the magnetic sensor module in the ST. In order to revolve the whole body frames, we used five-phase microstepping motor driver (MD5-HD14, Autonics, Gyeonggi-do, Korea) and five-phase stepping motor (A50K-M566-G10, Autonics). Its basic step angle was 0.72°/step and maximum speed at full step was 180 r/min. Using the stepping motor driver, we set the angular velocity of the calibration system to 1/120 RPS and we were able to obtain the angle with an accuracy of ±0.5 degree

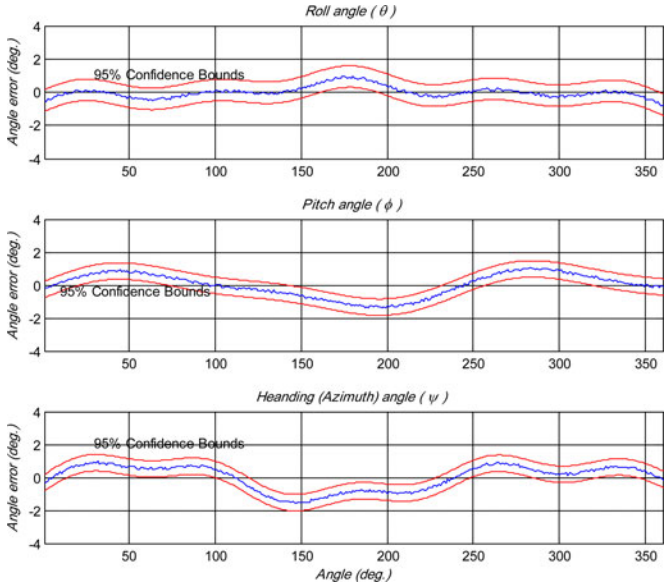


Fig. 8. Error tolerance of the proposed smart toothbrush system. The roll, pitch, and heading angles of ST were compared with the absolute angles of calibrator and the estimated angles by ST system.

Fig. 8 shows the difference error with respect to the absolute posture and it revealed that orientation error is less than $\pm 2^{\circ}$, and the tolerance of the ST system was considered appropriate for toothbrushing motion tracing.

### *B. Classification of Toothbrushing Regions*

Toothbrushing experiment was done at a washroom in our local facility. A bust mirror was located in front of the examinee, and he or she was asked not to move around and not to turn their heads while brushing. Sensor data from ST was transmitted wirelessly to the nearby computer for signal processing analysis. Fig. 9 shows the acquired signals including magnetic and accelerometer signals, roll, pitch, and heading angles during toothbrushing. Fig 10 shows the result of classified brushing regions.

After toothbrushing was completed, each posture segment that was classified by roll angle was reinspected based on the feature vectors by using (9). At first, the optimal number of clusters for each posture segment was estimated by using (12).

Next, for each cluster in a posture segment, further decision was made based on the criteria, as illustrated in Table II. For example, if a posture segment was defined as "BRUSH_LEFT," then there were three possibilities that the toothbrushing region would be AB side, left molar buccal side, or right molar lingual side, as described in Table II.

The average heading angle of ST for each cluster with respect to the heading direction of the front wall mirror was interpreted as a decision index. In addition, rolling-stroke direction was estimated in order to discriminate maxillary and mandibular regions and its direction was estimated by averaging roll angle values of each cluster. If the average roll angle was positive, we defined the bristle started from the maxillary region. We defined the bristle started from mandibular region if the average roll

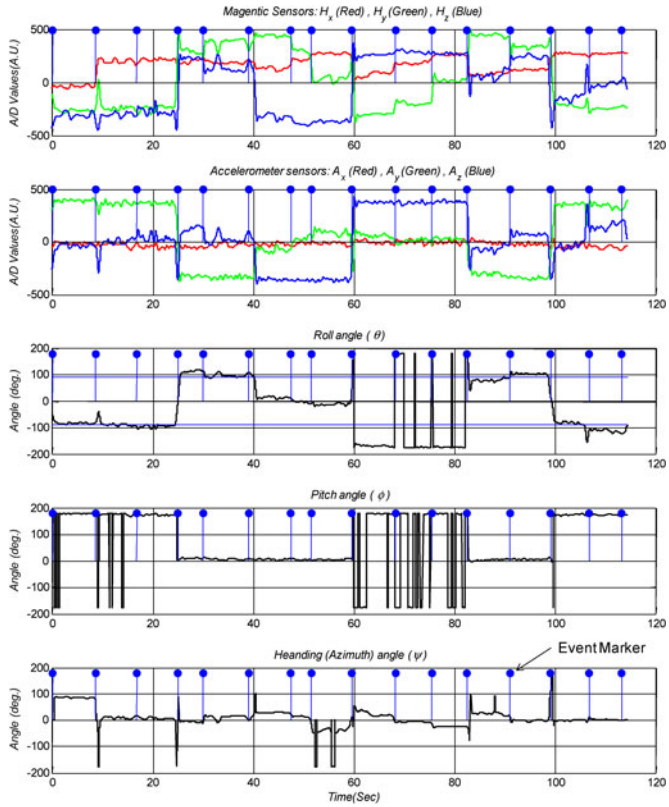


Fig. 9. Magnetic and accelerometer sensor signals of ST during toothbrushing (red solid line for $x$-axis, green "–" line for $y$-axis, and blue "-.-" line for $z$-axis). Filled circle (●) indicates the time-event marker.

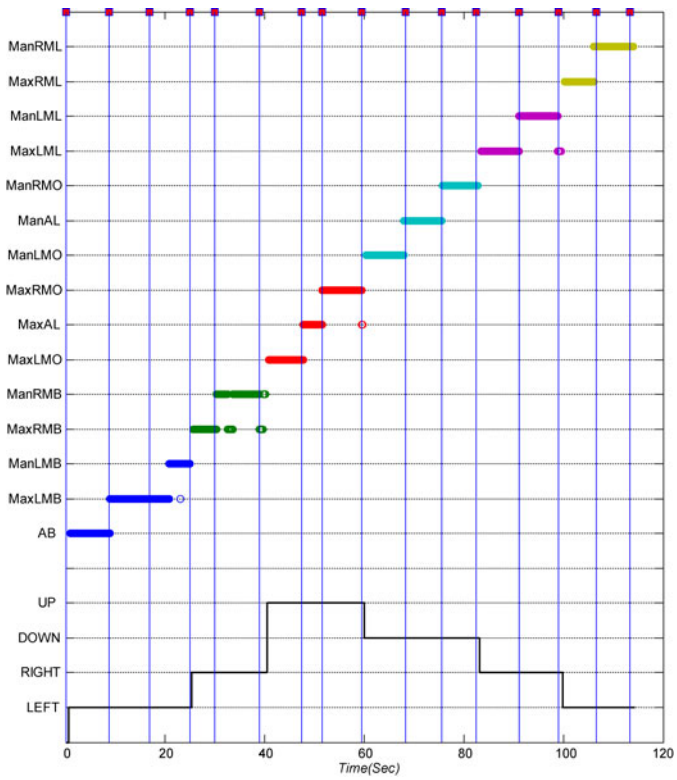


Fig. 10. Classification result of toothbrushing regions. The posture of toothbrush is illustrated at the bottom with a solid line. Filled circle (●) indicates the time-event marker.

TABLE III
RESULTS OF THE PROPOSED TOOTHBRUSH REGION DETECTION ALGORITHM

| | Subjects | | | | | | | | | | | | | | | Mean (sec) | STD |
|---|---|---|---|---|---|---|---|---|---|---|---|---|---|---|---|---|---|
| | 1 | 2 | 3 | 4 | 5 | 6 | 7 | 8 | 9 | 10 | 11 | 12 | 13 | 14 | 15 | | |
| AB* (sec) | 9 | 12 | 10 | 9 | 11 | 11 | 10 | 8 | 9 | 9 | 11 | 12 | 9 | 9 | 8 | 9.8 | 1.32 |
| MaxLMB (sec) | 6 | 7 | 9 | 8 | 9 | 8 | 9 | 7 | 8 | 7 | 8 | 8 | 7 | 9 | 10 | 8.0 | 1.07 |
| ManLMB (sec) | 5 | 9 | 8 | 7 | 7 | 8 | 7 | 6 | 8 | 6 | 6 | 7 | 7 | 9 | 8 | 7.2 | 1.15 |
| MaxRMB (sec) | 6 | 8 | 9 | 8 | 9 | 9 | 8 | 8 | 8 | 9 | 10 | 7 | 8 | 7 | 6 | 8.0 | 1.13 |
| ManRMB (sec) | 7 | 10 | 12 | 9 | 8 | 9 | 10 | 9 | 10 | 9 | 8 | 10 | 11 | 14 | 12 | 9.9 | 1.81 |
| MaxLMO (sec) | 10 | 9 | 9 | 9 | 10 | 10 | 11 | 9 | 9 | 10 | 8 | 10 | 11 | 9 | 9 | 9.5 | 0.83 |
| MaxAL (sec) | 7 | 9 | 10 | 8 | 8 | 9 | 9 | 10 | 9 | 9 | 8 | 7 | 11 | 9 | 9 | 8.8 | 1.08 |
| MaxRMO (sec) | 9 | 9 | 9 | 8 | 11 | 6 | 7 | 7 | 8 | 8 | 9 | 10 | 8 | 8 | 8 | 8.3 | 1.23 |
| ManLMO (sec) | 9 | 7 | 9 | 8 | 10 | 9 | 7 | 8 | 9 | 9 | 10 | 8 | 8 | 8 | 10 | 8.6 | 0.99 |
| ManAL (sec) | 8 | 9 | 9 | 7 | 8 | 8 | 9 | 10 | 11 | 8 | 8 | 7 | 8 | 8 | 9 | 8.5 | 1.06 |
| ManRMO (sec) | 9 | 10 | 9 | 8 | 8 | 9 | 11 | 9 | 8 | 7 | 8 | 9 | 8 | 7 | 8 | 8.5 | 1.06 |
| MaxLML (sec) | 7 | 8 | 9 | 8 | 8 | 9 | 10 | 10 | 8 | 9 | 9 | 8 | 7 | 8 | 10 | 8.5 | 0.99 |
| ManLML (sec) | 8 | 9 | 8 | 7 | 8 | 11 | 9 | 9 | 8 | 8 | 7 | 9 | 9 | 7 | 8 | 8.3 | 1.05 |
| MaxRML (sec) | 8 | 9 | 8 | 9 | 9 | 9 | 11 | 11 | 10 | 9 | 9 | 11 | 9 | 9 | 9 | 9.3 | 0.98 |
| ManRML (sec) | 9 | 10 | 10 | 9 | 12 | 11 | 10 | 7 | 8 | 9 | 9 | 8 | 8 | 9 | 9 | 9.2 | 1.26 |
| Total Brushing Time(Sec) | 122 | 138 | 142 | 127 | 139 | 138 | 142 | 132 | 134 | 128 | 130 | 135 | 135 | 135 | 137 | 134.3 | 5.64 |
| Total Regions | 7320 | 8280 | 8520 | 7620 | 8340 | 8280 | 8520 | 7920 | 8040 | 7680 | 7800 | 8100 | 8100 | 8100 | 8220 | 8056 | 338.3 |
| True Regions | 6997 | 8093 | 8261 | 7323 | 8151 | 8145 | 8262 | 7664 | 7842 | 7551 | 7675 | 7866 | 7765 | 7790 | 7977 | 7824 | 353.8 |
| False Regions | 323 | 187 | 259 | 297 | 189 | 135 | 258 | 256 | 198 | 129 | 125 | 234 | 335 | 310 | 243 | 231.9 | 69.6 |
| Accuracy (%) | 95.6 | 97.7 | 97.0 | 96.1 | 97.7 | 98.4 | 97.0 | 96.8 | 97.5 | 98.3 | 98.4 | 97.1 | 95.9 | 96.2 | 97.0 | 97.1 | 0.9 |

*Maxillary and Madibular anterior buccal sides are brushed with rolling stroke method. But it is difficult to discriminate the difference between maxillary and mandibular region clearly.
All abbreviations of each brushing regions are defined in Table II.

angle was negative. Combining the heading angle of ST, final brushing regions based on Table II were determined and each time period of position was calculated.

Overall results of 12 subjects are summarized in Table III. Total brushing regions were calculated by multiplying total brushing time and sampling rate since each sampled sensor data that is feature data is supposed to be in a certain region of dental arch, as illustrated in Fig. 1. Sampled feature data classified as not belonging to the appropriate region were regarded as false regions. The percentage of the exact recognition of brushing region over total regions was defined as the accuracy of brushing region detection.

Overall 97.1% ($\pm$0.91) of region detection accuracy was achieved in our investigation. In additions, each time period of all possible brushing positions are calculated. As for recognized brushing regions, among 16 possible toothbrushing regions, 14 brushing regions were clearly and reliably recognized except for the maxillary/mandibular AB regions. It is difficult to find any brushing differences in this region even though the rolling strokes method was used in different locations. Therefore, we classified these two regions as an AB region, resulting in 15 brushing regions in total.

## IV. DISCUSSION AND CONCLUSION

From our preliminary study [10], [11], several problems such as the ambiguity of the heading angle of ST while brushing inner tooth surfaces and the dip angle of magnetic sensor were identified. In this study, we successfully resolved these problems. In practice, it is difficult to calculate the exact dip angle, where toothbrushing is performed. Thus, if we know in advance which direction of ST is normal or parallel to the front reference, such as a front bust mirror, then we may neglect the heading error caused by missing the dip angle information. The solution to this issue might be to locate the electronic compass at the front reference; thus, we could automatically calibrate the initial position of ST.

Regarding the classification of the posture segments, in this study, we used a simple *k*-mean clustering method to explore whether the different heading periods exist in selected posture segments. Since there is a well-known problem regarding initial cluster centers, we equally divided the selected posture segment as the initial cluster centers by the optimal number of clusters calculated by using (12). Occasionally, subsegments, which have directional changes, are recognized as having only one cluster since the slow change of ST heading angle is not clearly classified. As summarized in Table III, most of false regions are caused by misclassified feature data and others are caused by posture transitions of the ST.

As for the brushing regions, even though subjects were asked to brush each region one at a time, it was difficult to discern the difference between maxillary and mandibular anterior regions. Because of the subject preference of brushing anterior buccal region with a single scrubbing up and down, ones toothbrushing habits are predominated with the preeducation effects before elementary school. This area is worthy of more experimental research.

The proposed ST system was able to effectively track toothbrushing regions and estimate the time duration of toothbrushing. In clinical application, brushing time is highly correlated with oral hygiene [22], [23] and plaque removal [24]. Therefore, the clinical relevance of our study is that an ST system integrated with motion sensors could provide a quantitative index for assessment of toothbrushing. Also, the improvement of classification algorithms would be helpful to define toothbrushing patterns more precisely, and eventually the proposed ST system would be effective in removing plaque and reducing occurrence of gum disease.

## REFERENCES

[1] U. Varshney, "Pervasive healthcare," *IEEE Computer*, vol. 36, no. 12, pp. 138–140, 2003.
[2] P. Bonato, "Wearable sensors/systems and their impact on biomedical engineering," *IEEE Eng. Med. Biol. Mag.*, vol. 22, no. 3, pp. 18–20, May/Jun. 2003.
[3] M. J. Cronin, W. Z. Dembling, M. A. Cugini, M. C. Thompson, and P. R. Warren, "Three-month assessment of safety and efficacy of two electric toothbrushes," *J. Dentistry*, vol. 33, no. Suppl. 1, pp. 23–28, 2005.

[4] S. L. Yankel and R. C. Emling, "Laboratory interproximal access efficacy comparison of bi-level and flat bristled toothbrushes," *J. Clin. Dentistry*, vol. 4, no. 4, pp. 128–130, 1994.
[5] D. W. Volpenhein, M. E. Walsh, P. A. Dellerman, and T. A. Burkett, "A new method for in-vitro evaluation of the interproximal penetration of manual toothbrushes," *J. Clin. Dentistry*, vol. 5, no. 1, pp. 27–33, 1994.
[6] H. R. Rawls, D. L. Lentz, G. W. Cobb, M. S. Bailey, J. Spencer, D. A. Williams, D. Walley, and J. Vidra, "Interproximal penetration of commercial toothbrushes as determined by static and dynamic tests using recommended brushing techniques," *J. Clin. Dentistry*, vol. 4, pp. 88–95, 1993.
[7] C. R. Allen, I. C. Leggett, and I. D. M. Macgregor, "Remote measurement of in-vivo toothbrushing forces as a clinical tool for dental hygiene purposes," in *Proc. IEEE Instrum. Meas. Technol. Conf.*, St. Paul, MN, May 1998, pp. 854–857.
[8] C. R. Allen, N. K. Hunsley, and I. D. M. Macgregor, "Development of a force-sensing toothbrush instrument using PIC micro-controller technology for dental hygiene," *Mechatronics*, vol. 6, no. 2, pp. 125–140, 1996.
[9] C. Poche, H. McCubbrey, and T. Munn, "The development of correct toothbrushing technique in preschool children," *J. Appl. Behav. Anal.*, vol. 15, no. 2, pp. 315–320, 1982.
[10] J. W. Lee, K. Lee, K. Lee, D. Kim, and K. Kim, "Development of smart toothbrush monitoring system for ubiquitous healthcare," in *Proc. 28th IEEE EMBS Annu. Conf.*, New York, 2006, pp. 6422–6425.
[11] K. H. Lee, J. W. Lee, K. S. Kim, D. J. Kim, K. H. Kim, H. K. Yang, K. S. Jeong, and B. C. Lee, "Tooth brushing pattern classification using three- axis accelerometer and magnetic sensor for smart toothbrush," in *Proc. 29th IEEE EMBS Annu. Conf.*, Lyon, France, 2007, pp. 4211–4214.
[12] K. R. Briting, *Inertia Navigation System Analysis*. Hoboken, NJ: Wiley, 1971.
[13] Y. F. Jiang, "Error analysis of analytic coarse alignment methods," *IEEE Trans. AES*, vol. 34, no. 1, pp. 334–337, Jan. 1998.
[14] S. P. Yoon and J. B. Lundberg, "Euler angle dilution of precision in GPS attitude determination," *IEEE Trans. AES*, vol. 37, no. 3, pp. 1077–1083, Jun. 2001.
[15] J. E. Lenz, "A review of magnetic sensors," *Proc. IEEE*, vol. 78, no. 6, pp. 973–989, Jun. 1990.
[16] M. J. Caruso, "Application of magnetoresistive sensors in navigation system," *Sens. Actuators, SAE SP-1220*, pp. 15–21, 1997.
[17] S. Y. Cho and C. G. Park, "Tilt compensation algorithm for 2-axis magnetic compass," *IEE Electron. Lett*, vol. 39, no. 22, pp. 1589–1590, Oct. 2003.
[18] S. Y. Cho and C. G. Park, "A calibration technique for a two-axis magnetic compass in telematics devices," *ETRI J.*, vol. 27, no. 3, pp. 280–288, 2005.
[19] J. B. MacQueen, "Some methods for classification and analysis of multivariate observations," in *Proc. 5th Berkeley Symp. Math. Statist. Probability*, vol. 1, Berkeley, CA, 1967, pp. 281–297.
[20] P. J. Rousseeuw, "Silhouettes: A graphical aid to the interpretation and validation of cluster analysis," *J. Comput. Appl. Math.*, vol. 20, pp. 53–65, 1987.
[21] D. W. Nunez, M. J. Fehrenbach, and M. Emmons, *Mosby's Dental Dictionary*, 2nd ed. New York: Elsevier, 2008.
[22] J. E. Clarkson, L. Young, C. R. Ramsay, B.C. Bonner, and D. Bonetti, "How to influence patient oral hygiene behavior effectively," *J. Dental Res.*, vol. 88, no. 10, pp. 933–937, 2009.
[23] J. E. Creeth, A. Gallagher, J. Sowinski, J. Bowman, K. Barrett, S. Lowe, K. Patel, and M. L. Bosma, "The effect of brushing time and dentifrice on dental plaque removal in vivo," *J. Dental Hygiene*, vol. 83, no. 3, pp. 111–116, 2009.
[24] K. Williams, A. Ferrante, K. Dockter, J. Haun, A. R. Biesbrock, and R. D. Bartizek, "One- and 3-minute plaque removal by a battery-powered versus a manual toothbrush," *J. Periodontol.*, vol. 75, no. 8, pp. 1107–1113, 2004.

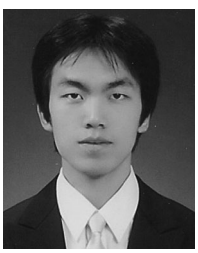

**Young-Jae Lee** (S'11) was born in Kyeonggi-do, Korea, in 1985. He received the B.S. and M.S. degrees in biomedical engineering from Konkuk University, Chungju, Korea, in 2008 and 2010, respectively, where he is currently working toward the Ph.D. degree in biomedical engineering.

His current research interests include biomedical instrument and development of ubiquitous healthcare device and sensor network, real-time digital signal processing, biomedical signal processing of electrocardiogram, motion sensing and pattern classification.

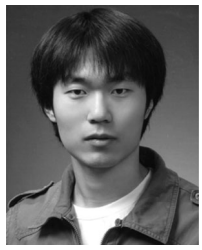

**Pil-Jae Lee** was born in Kyeonggi-do, Korea, in 1983. He received the B.S. degree in biotechnology from Sejong University, Seoul, Korea, in 2009. He is currently working toward the M.S. degree in biomedical engineering at Konkuk University, Chungju, Korea.

His current research interests include biomedical instrument, development of electromanometer and neural networks, interpolation algorithms, firmware, android application, and real-time digital signal processing.

**Kyeong-Seop Kim** received the B.S. and M.S. degrees in electrical engineering from the Yonsei University, Seoul, Korea, in 1979 and 1981, respectively, the M.Eng. degree in electrical engineering from Louisiana State University, Baton Rouge, in 1985, and the Ph.D. degree in electrical and computer engineering from the University of Alabama, Huntsville, in 1994.

From 1995 to 2001, he was a Principal Researcher of the Medical Electronics Laboratory, Samsung Advanced Institute of Technology, Kyounggi, Korea. Since March 2001, he has been a Faculty Member of the School of Biomedical Engineering, Konkuk University, Chungju, Korea. His research interests include medical image/signal processing, pattern recognition, and microwave radiothermometry for medical applications.

**Wonse Park** received the B.S. and M.S. degrees in oral and maxillofacial surgery from the College of Dentistry, Yonsei University, Seoul, Korea, in 1997 and 2006, respectively.

From 1997 to 2000, he was a Resident at Yonsei University Dental Hospital, where he studied oral and maxillofacial surgery. After completing his military service, he was a Fellow and Clinical Professor of oral and maxillofacial surgery at Yonsei University Dental Hospital.He is currently an Associate Professor of advanced general dentistry at the College of Dentistry, Yonsei University. His research interests include minor oral surgery, dental treatment of medically compromised patient, 3-D imaging analysis, computer-guided surgery, laser dentistry, and teledentistry.

**Kee-Deog Kim** received the D.D.S. degree and the M.S.D. and Ph.D. degrees in oral and maxillofacial radiology from Yonsei University, Seoul, Korea, in 1988, 1991, and 1997, respectively.

From 2002 to 2003, he was a visiting Professor in Department of Oral Pathology, Radiology & Medicine, The University of Iowa. Since 1996, he has been a Faculty Member of the College of Dentistry, Yonsei University, Seoul. His research interests include dental and medical informatics (picture archiving and communication system and electronic medical record), various image processing and digital technology application in oral and maxillofacial diagnostic science and dental treatment, and forensic and anthropologic radiology in association with human identification research.

**Dosik Hwang** received the B.S. and M.S. degrees in electrical engineering from Yonsei University, Seoul, Korea, in 1997 and 1999, respectively, and the Ph.D. degree in bioengineering from the University of Utah, Salt Lake City, in 2006.

From 2006 to 2008, he was a Researcher at the University of Colorado Health Science Center, Denver. He is currently an Assistant Professor at Yonsei University, Seoul, Korea. His research interests include biomedical signal processing, MRI, single-photon emission computed tomography, ultrasound imaging, computed-tomography reconstruction, biometrics, and computer-aided diagnosis.

**Jeong-Whan Lee** (S'95–M'99) was born in Seoul, Korea, in 1968. He received the B.S. and M.S. degrees in electrical engineering in 1992 and 1994, respectively, and the Ph.D. degree in electrical and computer engineering from the Yonsei University, Seoul, Korea, in 2000.

From 2000 to 2004, he was a Member of the Technical Staff of the Application Project Team and a Project Manager of the Ubiquitous-Health Project Team at the Samsung Advanced Institute of Technology, Kyounggi, Korea. Since September 2004, he has been a Faculty Member of the School of Biomedical Engineering, Konkuk University, Chungju, Korea. His research interests include biomedical signal processing and instrumentation, wearable/wireless devices for pervasive healthcare, sensing of vital signs/signatures, heart-rate variability, and biological signal measurements by electromagnetic waves and microwave radiothermometry.